# Can a droplet break up under flow without elongating? Fragmentation of smectic monodisperse droplets

L. Courbin,* W. Engl, and P. Panizza†
*Centre de Physique Optique Moléculaire Hertzienne UMR 5798, 351 Cours de la Libération, 33400 Talence, France*
(Received 17 December 2003; published 17 June 2004)

We study the fragmentation under shear flow of smectic monodisperse droplets at high volume fraction. Using small angle light scattering and optical microscopy, we reveal the existence of a break-up mechanism for which the droplets burst into daughter droplets of the same size. Surprisingly, this fragmentation process, which is *strain controlled* and occurs homogeneously in the cell, does not require any transient elongation of the droplets. Systematic experiments as a function of the initial droplet size and the applied shear rate show that the rupture is triggered by an instability of the inner droplet structure.

DOI: 10.1103/PhysRevE.69.061508 PACS number(s): 83.50.Xa, 83.50.Ax, 82.70.Uv

## INTRODUCTION

Dispersing two immiscible fluids requires mechanical mixing to rupture large droplets into smaller ones. The mechanism of fragmentation is therefore central to many industrial processes such as, for instance, painting, coating, and emulsions, since the mean droplet size controls the properties of the final material [1]. For simplicity's sake, since the pioneering work of Taylor [2], most studies have focused on the deformation and break up of isolated droplets at low Reynolds numbers. Under shear flow, the isolated droplet adopts an ellipsoidal shape at low flow strength. Rupture occurs when the capillary number, defined as the ratio of viscous to capillary forces, exceeds a critical value which depends on both $p$, the viscosity ratio between dispersed and continuous phases, and the nature of the flow [3–6]. At burst, the droplet draw ratio $D$, defined as the length required for break up over the original droplet size, is a function of $p$. For $p \leqslant 10^{-2}$, the droplet stretches continuously into long threads ($D \rightarrow \infty$) and breaks up in quiescent or sheared flow due to the growth of capillary-wave instabilities [7], or other processes such as tip streaming [2–4,8] or end pinching [9,10]. For $10^{-2} \leqslant p \leqslant 2$, the droplet elongation is less pronounced but still important ($D \approx 3-4$) and break up occurs by fracture, whereas for $p \geqslant 4$, the droplet deformation remains modest and no break up is observed under shear flow.

However, in industrial processes, mechanical mixing usually involves high droplet volume fractions where both droplet break up and coalescence may occur [11]. In addition, for a wide class of materials such as, for instance, polymer dispersed liquid crystals, liquid crystal emulsions, multiple emulsions, or multilamellar liposomes, the droplets present some internal hydrodynamic modes which may alter their response to deformation and burst. Yet, despite their importance, these two aspects still remain largely undocumented in the literature.

In the present work, we investigate the fragmentation of smectic droplets under shear flow and report on a rupture process that *does not require any droplet stretching*. This phenomenon occurs homogeneously in the cell: each initial droplet bursts out identically into daughter droplets of same size. We show that the origin of this mechanism likely rises from an instability of inner lamellar structure of the droplets.

We study a pseudobinary mixture made of 20 wt % sodium bis(2-ethylhexyl) sulfo-succinate (AOT) and 80 wt % brine with a sodium chloride content of $S = 1.6$ wt %. At $T = 25\ ^\circ$C, the solution phase-separates into a lamellar ($L_\alpha$) and a sponge ($L_3$) phase with 90% and 10% as the respective volume fractions [12]. Although both coexisting phases are made of the same AOT bilayers, their long-range structure differs. In the birefringent $L_\alpha$ phase, the bilayers periodically stack along one direction with a smectic order, whereas in the isotropic $L_3$ phase, they randomly connect and divide space in two equivalent subvolumes of solvent [13]. Under flow, this two-phase mixture is well known to form monodisperse multilamellar droplets immersed in the $L_3$ matrix. At low shear rates, one finds the so-called "closed compact Taylor droplets" whose size varies as the inverse of shear rate, $\dot{\gamma}^{-1}$, and results from a mechanical balance between viscous stress and Laplace pressure [14]. Above a critical shear rate ($\dot{\gamma}_c \approx 25\ \mathrm{s}^{-1}$), these droplets organize into a sixfold colloidal crystal (see Fig. 1). Since the steady state droplets are monodisperse, this system therefore offers a unique way to investigate how in a close compact assembly made of smectic droplets the fragmentation process depends on their initial size and on the applied shear rate. Moreover, because of the near optical index matching between both phases, the temporal variation of the mean droplet size under flow can directly be accessed by small angle static light scattering (SALS).

## EXPERIMENTS

Shear experiments are performed with a house-made Couette cell, consisting of two concentric glass cylinders with gap $e = 1$ mm. The inner cylinder $R_{\mathrm{in}}$ remains fixed while the outer one (radius $R_{\mathrm{out}} = 16$ mm) rotates. The angular velocity of the rotor is controlled by a computer. A circularly polarized laser beam (He-Ne, $\lambda = 632.8$ nm in vacuum) passes

*Electronic address: l.courbin@cpmoh.u-bordeaux1.fr
†Electronic address: p.panizza@cpmoh.u-bordeaux1.fr

 

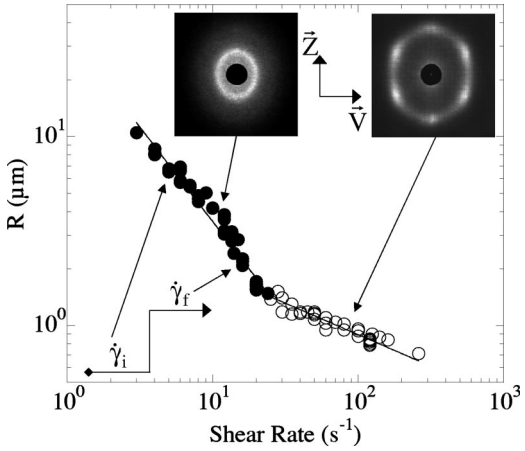


FIG. 1. Variation of steady droplet size with shear rate: glassy state (●) and colloidal crystal (○). Insets: shown are the SALS patterns in the (**v**,**z**) plane corresponding to the two distinct steady regimes, and a schematic representation of the applied shear step.

through the cell in only one of the gaps along $\nabla v$, the shear gradient direction. The unpolarized light scattered in the velocity-vorticity plane (**v**,**z**) is observed on a screen and digitalized by means of charge-coupled device camera for frame acquisition.

## RESULTS

In order to study the fragmentation of droplets, we first prepare an initial steady state at constant shear rate $\dot{\gamma}_i$ and then abruptly increase the shear rate to a new value $\dot{\gamma}_f$. Depending on the value of $\Delta\dot{\gamma}=\dot{\gamma}_f-\dot{\gamma}_i$, the shear step change, two distinct kinetic processes can be distinguished (Fig. 2).

When $\Delta\dot{\gamma}$ is small, the radius of the scattering ring increases continuously to its final value (Fig. 3) indicating that the mean droplet size decreases. Microscopic observations between crossed polarizers reveal that (1) this process occurs homogeneously in the cell and (2) the size distribution remains very narrow throughout this kinetic process. These two observations prove that the number of layers for each initial droplet must decrease continuously. This may occur either by peeling if permeation is too slow or, as suggested

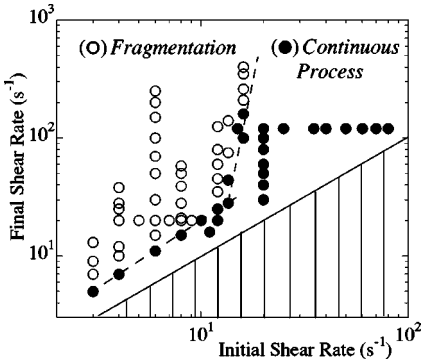


FIG. 2. Dynamical diagram representing the nature of the kinetic process as a function of $\dot{\gamma}_i$ and $\dot{\gamma}_f$: continuous (●); fragmentation (○). The striped area stands for $\dot{\gamma}_i \geqslant \dot{\gamma}_f$.

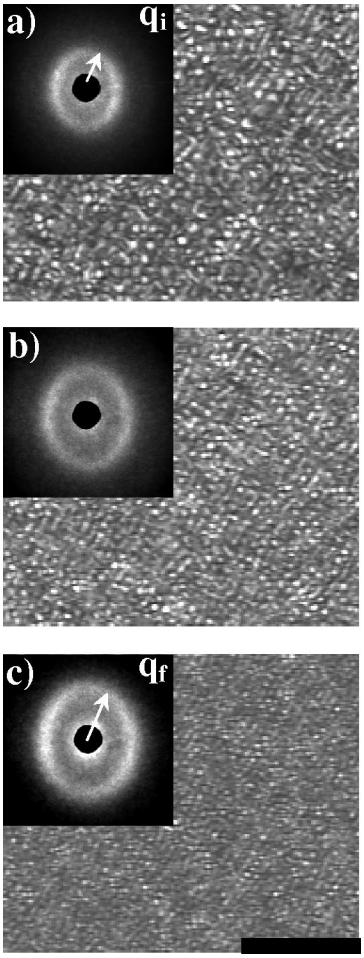


FIG. 3. Temporal evolution of the texture observed between crossed polarizers and of the corresponding SALS pattern in the (**v**,**z**) plane (insets), for a continuous process: (a) $t=0$ s, (b) $t=270$ s, and (c) $t=18\,000$ s. The origin of time corresponds to the change in the applied shear rate. The values of $\dot{\gamma}_i$ and $\dot{\gamma}_f$ are, respectively, $\dot{\gamma}_i=8$ s$^{-1}$ and $\dot{\gamma}_f=15$ s$^{-1}$. The length of the black bar indicates 50 $\mu$m.

by Prost *et al.*, by release of matter (first solvent and then surfactant) from the center to the outside of droplets when permeation is faster [16,17]. To clarify this point, a systematic investigation of this process as a function of experimental parameters is currently under way and will be published in a forthcoming paper. For now, in the present text, we will refer to this process as *continuous*.

When $\Delta\dot{\gamma}$ is larger, the evolution of the SALS pattern drastically differs (Fig. 4). First, the intensity of the initial scattering ring decreases and then, after a well defined delay time $t_r$, a scattering ring suddenly emerges at a larger wave vector $q=q_r$. Then the position of this ring moves continuously toward larger wave vectors until it reaches its steady state value $q=q_f$. For $t\leqslant t_r$, in the whole shear cell, the texture exhibits a well defined modulation of the refractive index. This modulation, which is identical to that observed at $t=0$ s for the initial assembly made of monodisperse multilamellar droplets, indicates that the structure factor of the droplets does not change during this first step. Therefore, the turbidity enhancement of the solution and the intensity de-

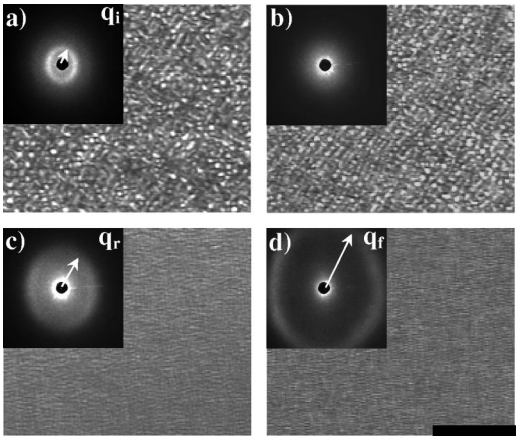


FIG. 4. Temporal evolution of the texture observed between crossed polarizers and of the corresponding SALS pattern in the $(\mathbf{v},\mathbf{z})$ plane (insets), for a fragmentation process: (a) $t=0$ s, (b) $t=60$ s, (c) $t=110$ s, and (d) $t=17\,000$ s. The origin of time corresponds to the change in the applied shear rate. The values of $\dot{\gamma}_i$ and $\dot{\gamma}_f$ are, respectively, $\dot{\gamma}_i=8\ \mathrm{s}^{-1}$ and $\dot{\gamma}_f=50\ \mathrm{s}^{-1}$. The length of the black bar indicates 50 $\mu$m.

crease of the SALS ring occurring for $t \leqslant t_r$ likely result from a modification of the optical contrast between the smectic droplets and the continuous medium ($L_3$ phase). This probably occurs through release of water by the droplets [18,19]. At $t \approx t_r$, the texture still presents a homogeneous modulation of the optical index in the whole cell. However, the characteristic wavelength of this modulation is much smaller, indicating that all initial droplets have fragmented into daughter droplets of quasi-identical size.

At this stage, one can definitely assert that this rupture process is very different from what is reported in the literature [3–10] since *it does not involve any transient stretching of the initial droplets*. An excellent proof of this is given in our time resolved SALS experiments by the absence of any large anisotropy of the scattering pattern. Thus, contrary to what is observed in emulsions, we do not witness a vertical streak [21,22] characteristic of the formation of transient long threads aligned along the flow direction. Note that a close look at our SALS patterns, however, reveals a small anisotropy of about 10%. Nevertheless, if the same experiment is performed with a plate to plate cell no such effect is noticeable. The corresponding SALS pattern is an isotropic ring. This experimental fact clearly proves that the anisotropy observed in Fig. 3 and Fig. 4 results from optical distortion due to our cylindrical Couette geometry and not from a flow effect. After the fragmentation has occurred (i.e., for $t \geqslant t_r$), the mean droplet size decreases continuously toward its final value. Through this secondary process, the texture remains homogeneous in the cell and the droplet size distribution remains very narrow. These observations suggest that once the initial droplets have ruptured, the daughter droplets do not fragment any longer and relax to their final size according to the same *continuous process*, (i.e., peeling or slow matter release from the center to the outside droplets) that we previously quoted.

In order to gain more insights into the exact nature of the fragmentation process, we perform a systematic study of the

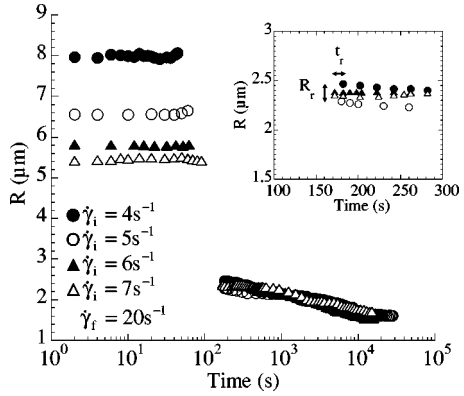


FIG. 5. Variation of the droplet size $R$ with time for different values of the initial shear rates: $\dot{\gamma}_i=4\ \mathrm{s}^{-1}$ (●), $\dot{\gamma}_i=5\ \mathrm{s}^{-1}$ (○), $\dot{\gamma}_i=6\ \mathrm{s}^{-1}$ (▲), and $\dot{\gamma}_i=7\ \mathrm{s}^{-1}$ (△). The values of the final shear rate and size are, respectively, $\dot{\gamma}_i=20\ \mathrm{s}^{-1}$ and $R_f \approx 1.6$ $\mu$m. One finds $R_r=2.35\pm0.10$ $\mu$m and $t_r=175\pm5$ s.

fragmentation time $t_r$ and size $R_r$ as a function of the initial droplet size $R_i$ (Fig. 5) and of the final shear rate $\dot{\gamma}_f$ (Fig. 6).

The rupture time $t_r$ varies as $\dot{\gamma}_f^{-1}$, indicating that the fragmentation of droplets is a *strain controlled* process (Fig. 7). Surprisingly, the value of the critical rupture strain necessary for the initial droplets to rupture (i.e., $\gamma_r=\dot{\gamma}_f t_r \approx 4200$) is very large and independent of $R_i$ (see Fig. 5). In other words, the droplet fragmentation occurs when the number of rotations of the rotor reaches the critical number $N_r \approx 42$, whatever the initial size is.

Now, let us focus on the value of the droplet size obtained after the fragmentation. It can roughly be estimated using SALS through the relation $R_r=2\pi/q_r$ [20]. Our results show that it does not depend on $R_i$ (see Fig. 5) and varies with $\dot{\gamma}_f$ according to $R_r \propto \dot{\gamma}_f^{-1/3}$ (see Fig. 7).

This value is identical to the size of the initial droplets obtained when one shears the premixed $L_\alpha$-$L_3$ two-phase mixture at $\dot{\gamma}_f$ (Fig. 8 and Fig. 9). In such an experiment, at $t=0$ s, the premixed mixture is introduced into the Couette cell and then sheared at $\dot{\gamma}_f$. As previously published [15], after a well defined delay time $t=t_{em}$, we observe in SALS

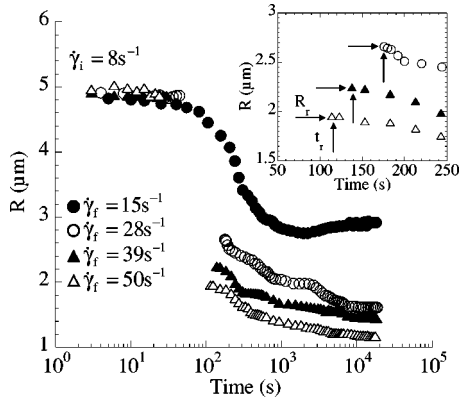


FIG. 6. Variation of the droplet size $R$ with time for different values of the final shear rates: $\dot{\gamma}_f=15\ \mathrm{s}^{-1}$ (●), $\dot{\gamma}_f=28\ \mathrm{s}^{-1}$ (○), $\dot{\gamma}_f=39\ \mathrm{s}^{-1}$ (▲), and $\dot{\gamma}_f=50\ \mathrm{s}^{-1}$ (△). The values of the initial shear rate and size are, respectively, $\dot{\gamma}_i=8\ \mathrm{s}^{-1}$ and $R_i \approx 4.8$ $\mu$mm.

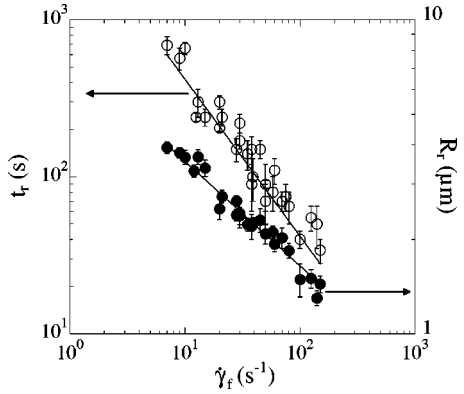


FIG. 7. Variation of the fragmentation time $t_r$ and droplet size $R_r$ as functions of $\dot{\gamma}_f$. The best power law fits give $t_r=(4186\pm95)/\dot{\gamma}_f$ and $R_r=(7.6\pm0.1)\dot{\gamma}_f^{-1/3}$.

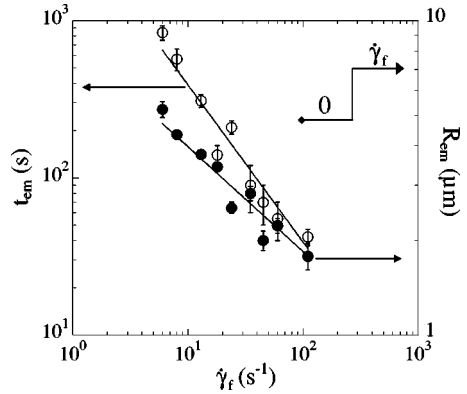


FIG. 9. Variation of the emergence time $t_{em}$ and droplet size $R_{em}$ as functions of the shear rate $\dot{\gamma}_f$ and a schematic representation of the applied shear step. The best power law fits give $t_{em}=(3912\pm181)/\dot{\gamma}_f$ and $R_{em}=(8.6\pm0.1)\dot{\gamma}_f^{-1/3}$.

the sudden emergence at $q_{em}$ of a scattering ring which allows us to estimate the size $R_{em}$ of the small monodisperse droplets that are formed. Moreover, both times $t_{em}$ and $t_r$ are comparable (see Fig. 7 and Fig. 9).

## DISCUSSION

After reaching the critical strain, the initial droplets become unstable and burst into daughter droplets of almost the same size. Within this picture, it is therefore reasonable to think that the size after fragmentation corresponds to the most unstable wavelength $\Lambda$ of an instability occurring within each initial droplet. Let us try to discuss a possible physical mechanism for this instability monitoring the fragmentation process. As revealed by the turbidity enhancement observed for $t\leqslant t_r$, water is likely released from the droplets due to the pressure increase resulting from the shear step. Such a phenomenon has already been observed in a few lamellar phases [18] and has also been recently invoked to explain droplet size oscillations occurring in some $L_\alpha$-$L_3$ two-phase mixtures [19]. As a result of this water release, the droplet volume changes, whereas the number of surfactant molecules remains unchanged. Therefore, the droplets, which are now under stress, have to find a way to accommodate this new membrane excess area. This can be done by either (1) increasing the number of layers, or (2) keeping the number of layers constant but (i) releasing surfactant molecules in the continuous phase or (ii) buckling the membranes. Our experiment suggests that, when the release of water is high enough, a buckling instability will likely develop within each droplet leading further to its fragmentation (see Fig. 10).

We believe a similar mechanism occurs upon sonication, since large amplitude undulations in the bilayers of sonicated liposomes have been witnessed by Zasadzinski [23].

Now our observations show that the variation of $\Lambda$ with $\dot{\gamma}_f$ is similar to that observed for the most unstable wave vector $q_{em}$ monitoring the emergence of multilamellar vesicles upon shearing oriented lamellar phases [24]. We do

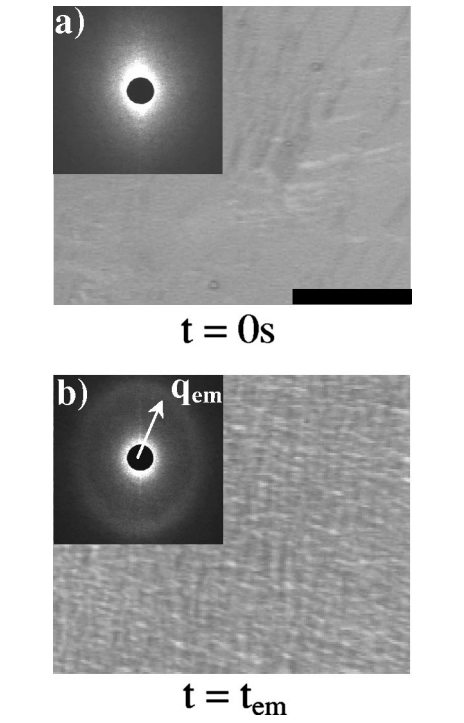


FIG. 8. Temporal evolution of the texture observed between crossed polarizers and of the corresponding SALS pattern in the $(\mathbf{v},\mathbf{z})$ plane (insets), obtained upon shearing the $L_\alpha/L_3$ mixture: (a) $t=90$ s and (b) $t=t_{em}=270$ s. The origin of time is taken once the shear rate $\dot{\gamma}_f=12$ $s^{-1}$ is applied. The length of the black bar indicates 50 $\mu$m.

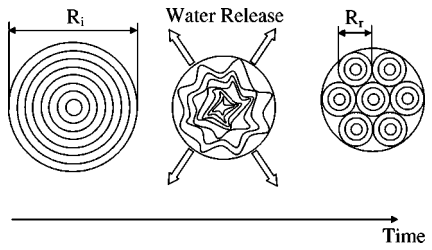


FIG. 10. Schematic representation of a possible scenario yielding the fragmentation process.

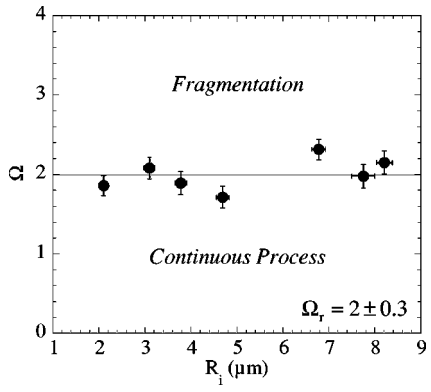


FIG. 11. Dynamical diagram written in terms of $R_i$ and $\Lambda$.

not have an explanation for this similarity and for the fact that both phenomena are strain controlled. However, one can note that they both seem triggered by the need to accommodate an excess surface area, although its origin differs. For oriented lamellar phases, the excess surface area originates from the suppression by the shear flow of the thermal undulations of the membranes as suggested by [25,26], whereas here it results from the water release (i.e., compression) of the droplets.

Finally, let us analyze the dynamical diagram (see Fig. 2) which represents the nature of the rupturing process (fragmentation or continuous) as a function of $\dot{\gamma}_i$ and $\dot{\gamma}_f$, now in terms of $R_i$ and $\Lambda$ (Fig. 11).

As shown in this figure, the nature of the kinetics process is controlled by the ratio $\Omega = R_i/R_r = R_i/\Lambda$. When $\Omega \leqslant \Omega_r$, where $\Omega_r = 2$, the size of the initial droplets decreases continuously, whereas for $\Omega \geqslant \Omega_r$, the droplets suddenly burst out. A criterion for droplet break up (i.e., a *discontinuous process*) to occur is therefore that the initial droplet size be at least twice larger than $\Lambda$ (i.e., $\Omega = \Omega_r = 2$), the most unstable wavelength of the fragmentation instability. In other words, multilamellar droplets can never fragment into fewer than eight daughter droplets.

As a final comment, let us point out that our burst mechanism via lamellar buckling implies a compression induced release of water from the droplets. For isolated droplets, such a pressure change in shear flow is intrinsically anisotropic and should result in elongation along the 45° direction to the flow, and compression along the 135° direction. Consequently, in our experiments where the droplets are closed compact, the absence of such elongation suggests that mechanical interaction between droplets plays an essential role in the burst phenomenon. To conclude, we believe that this present work sheds light on the importance of both the volume fraction and the internal structure of droplets in understanding their fragmentation under flow and therefore also predicting and controlling their final properties.

## ACKNOWLEDGMENTS

It is a pleasure to thank T. Bickel, A. Colin, D. Roux, F. Nallet, and A. Wurger for fruitful discussions and T. Douar and M. Winckert for technical assistance. CPMOH is UMR 5798 of the CNRS, associated with University Bordeaux I. This work was supported by the Conseil Régional d'Aquitaine (CTP Grant No. 980209202).

[1] R. G. Larson, *The Structure and Rheology of Complex Fluids* (Oxford University Press, Oxford, 1999).
[2] G. I. Taylor, Proc. R. Soc. London, Ser. A **146**, 501 (1934).
[3] H. P. Grace, Chem. Eng. Commun. **14**, 225 (1982).
[4] W. Bartok and S. G. Mason, J. Colloid Sci. **14**, 13 (1959);P. D. Rumscheidt and S. G. Mason, *ibid.* **16**, 210 (1961).
[5] B. G. Bentley and L. G. Leal, J. Fluid Mech. **167**, 241 (1986).
[6] For a review, see J. M. Rallison, Ann. Rev. Fluid Chem. **16**, 45 (1984).
[7] L. Rayleigh, Proc. London Math. Soc. **10**, 4 (1878).
[8] S. Torza, R. G. Cox and S. G. Mason, J. Colloid Interface Sci. **38**, 395 (1972).
[9] H. A. Stone, B. J. Bentley, and L. G. Leal, J. Fluid Mech. **173**, 131 (1986).
[10] H. A. Stone and L. G. Leal, J. Fluid Mech. **198**, 399 (1989).
[11] J. Bibette, F. Leal Calderon, V. Schmitt, and P. Poulin, *Emulsion Science, Basic Principles, an Overview* (Springer-Verlag, Berlin, 2002);T. G. Mason and J. Bibette, Phys. Rev. Lett. **77**, 3481 (1996).
[12] O. Gosh and C. A. Miller, J. Phys. Chem. **91**, 258 (1987).
[13] D. Roux, C. Coulon, and M. E. Cates, J. Phys. Chem. **91**, 258 (1992).
[14] L. Courbin, G. Cristobal, J. Rouch, and P. Panizza, Europhys. Lett. **55**, 880 (2001).
[15] L. Courbin, R. Pons, J. Rouch, and P. Panizza, Europhys. Lett. **61**, 275 (2003).
[16] J. Prost, S. Leibler, and D. Roux (unpublished).
[17] P. Panizza, A. Colin, C. Coulon, and D. Roux, Eur. Phys. J. B **4**, 65 (1998).
[18] J. Leng, F. Nallet, and D. Roux, Eur. Phys. J. E **4**, 337 (2001).
[19] L. Courbin, P. Panizza, and J.-B. Salmon, Phys. Rev. Lett. **92**, 018305 (2004).
[20] L. Courbin and P. Panizza, Phys. Rev. E **69**, 021504 (2004).
[21] T. Hashimoto, K. Matsuzaka, E. Moses, and A. Onuki, Phys. Rev. Lett. **74**, 126 (1995).
[22] C. Mabille, F. Leal Calderon, J. Bibette, and V. Schmitt, Europhys. Lett. **61**, 708 (2003).
[23] J.-A.-N Zasadzinski, Biophys. J. **49**, 1119 (1986).
[24] L. Courbin, J.-P. Delville, J. Rouch, and P. Panizza, Phys. Rev. Lett. **89**, 148305 (2002).
[25] A. G. Zilman and R. Granek, Eur. Phys. J. B **11**, 593 (1999).
[26] S. W. Marlow and P. D. Olmsted, Eur. Phys. J. E **8**, 485 (2002).